Hindawi
Geofluids
Volume 2017, Article ID 4126908, 8 pages
https://doi.org/10.1155/2017/4126908

Research Article

Investigating the Permeability of Marble under Moderate Pressure and Temperature

Jianping Yang,[1] Weizhong Chen,[1,2] Diansen Yang,[1] and Hongming Tian[1]

[1]*State Key Laboratory of Geomechanics and Geotechnical Engineering, Institute of Rock and Soil Mechanics, Chinese Academy of Sciences, Wuhan 430071, China*
[2]*Research Center of Geotechnical and Structural Engineering, Shandong University, Jinan 250061, China*

Correspondence should be addressed to Diansen Yang; dsyang@whrsm.ac.cn

Received 8 May 2017; Revised 21 July 2017; Accepted 7 August 2017; Published 11 September 2017

Academic Editor: Qinghui Jiang

The permeability of intact marble samples collected from the depth of 1.6 km in southwestern China is investigated under moderate confining pressures and temperatures. No microcracks initiate or propagate during the tests, and the variation of permeability is due to the change of aperture of microcracks. Test results show a considerable decrease of permeability along with confining pressure increase from 10 to 30 MPa and temperature increase from 15 to 40°C. The thermal effect on the permeability is notable in comparison with the influence of the stress. A simple permeability evolution law is developed to correlate the permeability and the porosity in the compressive regime based on the microphysical geometric linkage model. Using this law, the permeability in the compressive regime for crystalline rock can be predicted from the volumetric strain curve of mechanical tests.

1. Introduction

The transport properties of rocks are of significant importance for many topics of earth sciences, for example, exploration and production of hydrocarbons, oil/gas storage in deep cavern, and high-level radioactive nuclear waste geological disposal [1–4]; they are also vital to understand the fundamental geologic processes such as heat and mass transfer, earthquake, and metamorphism [5–9]. Permeability is a key parameter to describe the transport properties of materials and it can be measured using different methods, for example, steady method and pulse-test [10]. Due to Klinkenberg effect, the measured apparent gas permeability for tight rock is often different from the intrinsic permeability, which is related solely to the pore geometry (e.g., porosity, pore shape, and pore-size distribution) of the rock and is independent of the properties of the fluid. In the following texts, the term *permeability* is used to represent *intrinsic permeability* for brevity.

Several factors, for example, stress level, chemical effects, and temperature, can influence rock permeability by changing the pore geometry of the material [11–17]. These factors can significantly change the permeability of rock sample. For instance, Souley et al. [18], Schulze et al. [19], Jiang et al. [20], and Chen et al. [4] investigated the permeability change due to mechanical loading, and they found that the microcrack growth can result in an increase of permeability for 3~5 orders of magnitudes. Many studies focused on the thermal effects on rock permeability subjected to high temperatures (>100°C) [13, 21–24]. For instance, Zharikov et al. [23] studied the permeability of amphibolite collected from Kola surface, Kola superdeep borehole (at depth of 11.4 km), and KTB borehole (at depth of 3.8 km) at temperatures up to 600°C. It was found that the permeability decreased first and then re-increased while the temperature exceeded 300°C during heating at low confining pressure (30–80 MPa). Microstructure investigations and analysis showed that the increase of rock matrix compressibility reduces the microcracks apertures from 100 to 300°C, and it leads to the decrease of the permeability. While temperature was higher than 300°C, the intensive microcrack generated by heat cracking at mineral grain boundaries was responsible to the increase of the permeability.

Compared with the extensive studies on permeability evolution in the dilatant regime and high temperatures which can result in generation and propagation of microcracks, few

Table 1: Test results on flow rate of sample D20 in different conditions.

Sample D20: oil temperature: 14.5°C, room temperature: 16.0°C					
10 MPa		20 MPa		30 MPa	
Inlet gas pressure/MPa	Flow velocity/(10^{-3} mL·s^{-1})	Inlet gas pressure/MPa	Flow velocity/(10^{-3} mL·s^{-1})	Inlet gas pressure/MPa	Flow velocity/(10^{-3} mL·s^{-1})
1.95	0.00145	2.8	0.00175	2.97	0.00135
3	0.0025	4	0.00284	3.98	0.00196
4.04	0.00391	4.98	0.00392	4.95	0.00265
5.1	0.00595	5.99	0.00515	5.94	0.00348
6.1	0.00806	6.92	0.00645	6.96	0.00446
7.05	0.0101				

permeability tests and analysis have been performed under moderate temperatures in the compressive regime. However, the permeability variation of rock material under moderate pressures and temperatures is of great importance in some cases, for example, fluid movement at the shallow depth of the crust [25], long-term performance of an underground nuclear waste repository constructed in crystalline rock [3], weathering action of building claddings, and historical monuments due to seasonal temperature changes [26]. In this study, the transport properties of intact marble collected at depth of 1.6 km are measured under moderate temperatures and confining pressures. To explain the experimental results, a simple formula correlating permeability with porosity is proposed based on a penny-shaped crack linkage model. The applicability of the formula is verified against the measured results.

2. Tested Material and Experimental Procedure

2.1. Tested Material. The tested material was taken from the diversion tunnel at the depth of 1600 m of the JinPing hydropower station in southwestern China. To measure the permeability under moderate temperature, two cylindrical samples (D20 and D30) with a diameter of 49.1 mm and a length of 80.0 mm were drilled from the same block. There are no preferred fabric textures of the tested material. The sample axes are parallel to the vertical axis of the ground. The density of the dry sample is 2.76 kg/m^3, Young's modulus is between 45 GPa and 60 GPa at high confining pressures (40 MPa to 60 MPa), and the uniaxial compressive strength is 103 MPa. The results of mineral X-ray diffraction show that the material consists of calcite (8.6% in weight), dolomite (91.0%), and mica (0.4%) [27].

The microstructure of the material has been investigated using optical microscopy and scanning electron microscopy (SEM). From the optical images examined under plane polarized light (Figure 1(a)), it can be seen that there is no preferred orientation of the minerals. The mineral sizes are mostly among 0.2 to 0.5 mm, and the transport path of fluid is mainly the interface of the grains. The parallel lines inside grains are the cleavage of calcite. The SEM images (Figure 1(b)) show that the rock is extremely compact. The grain boundaries in the SEM picture can only be distinguished by the variation of cleavage direction. The pore size and porosity of the marble are evaluated using mercury intrusion porosimetry. The porosities of the two samples are 0.17% and 0.14%, respectively. The pore size of the material mainly varies between 40 nm and 400 nm (Figure 2). It is close to the results of Italy and Sweden marble, in which the pore-size distributions cover a range of 2–200 nm [28].

2.2. Experimental Procedure. The steady-state gas flow method is employed to investigate the transport property of the intact marble. The inlet gas pressure is maintained during the permeability test and the outlet pressure is the atmosphere pressure. A high-precision bubble gas flow meter is used to measure the flow rate of the outlet gas. The temperature is controlled using a heating system mounted around the sample cell. To seal the sample, a thin inner casing (nitrile butadiene rubber, thickness 0.3 mm) and a thick outer casing (thick Viton jacket, thickness 7 mm) are coated to prevent the oil from leaking into the sample. The likelihood of bypass flow that could take place at the interface between the sample and the inner casing may enlarge the flow rate substantially for tight rock [26]. In this study, liquid silica rubber (LSR) is used to stick the sample and inner casing together to eliminate the bypass flow.

Before permeability tests, the specimens were dried at 105°C in a vacuum oven for 24 hr. The sample D20 was tested under the hydrostatic pressures of 10, 20, and 30 MPa at room temperature (16°C), while the sample D30 under the constant pressure of 20 MPa was tested at the successively increasing temperature, that is, 15, 30, and 40°C. Several gas pressure levels were chosen to estimate the possible Klinkenberg effect.

When the gas permeability measurement is finished, the sample D20 was then put in MTS to measure the volume strain under the same mechanical loading conditions. Note that the low hydrostatic stress will not induce any damage of the sample.

3. Experimental Results

The steady gas flow velocity and the corresponding test conditions of the samples D20 and D30 are listed in Tables 1 and 2, respectively.

Due to small pore size, Klinkenberg effect could not be ignored during gas permeability measurement. Klinkenberg

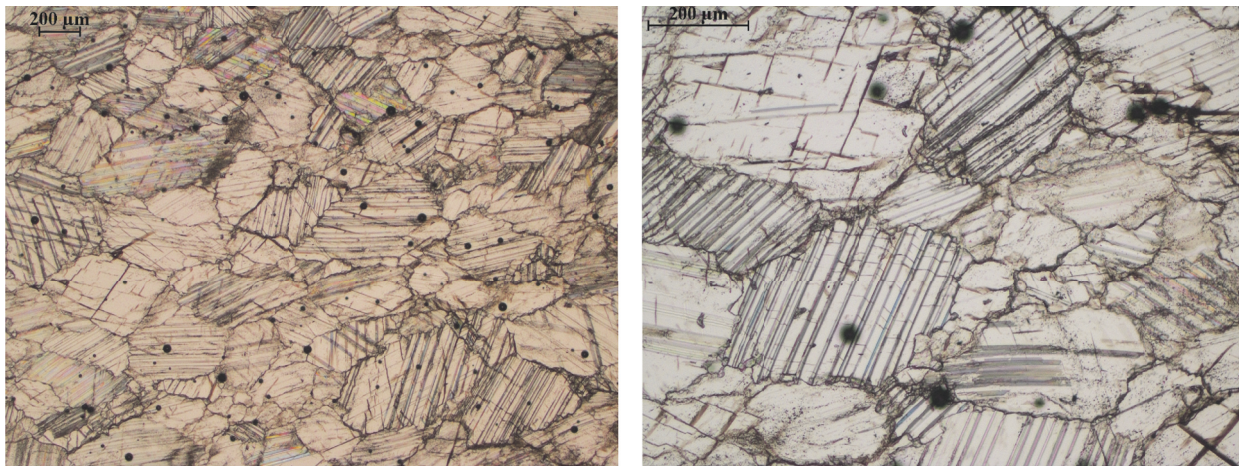

(a) Pictures under optical microscope

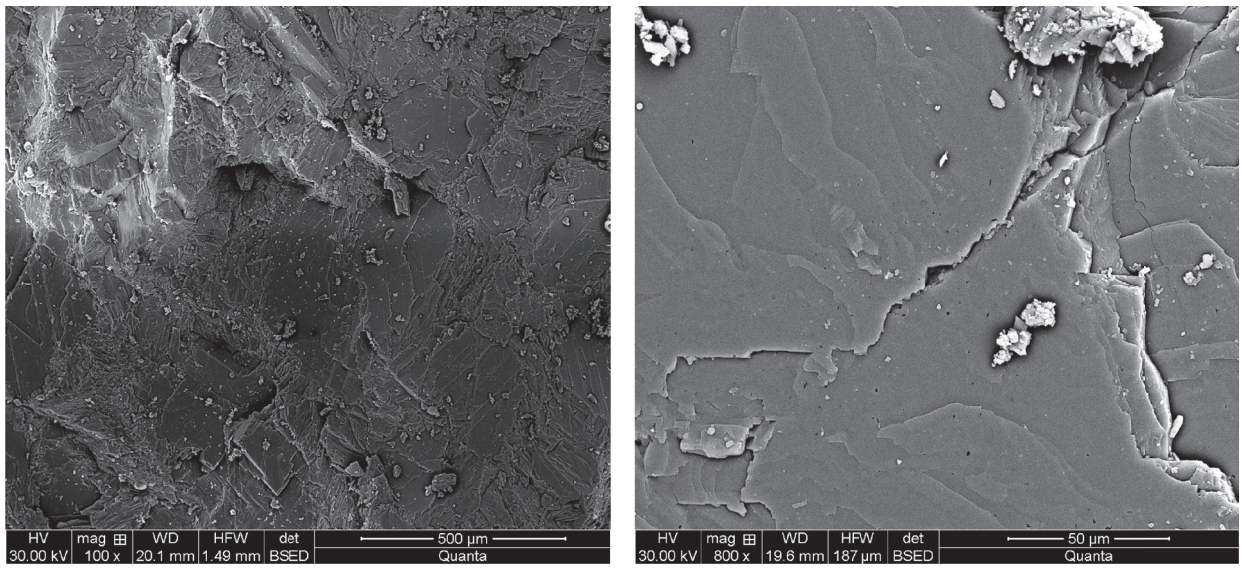

(b) Pictures under SEM

Figure 1: Microstructure of the Jinping marble investigated by optical microscopes and SEM.

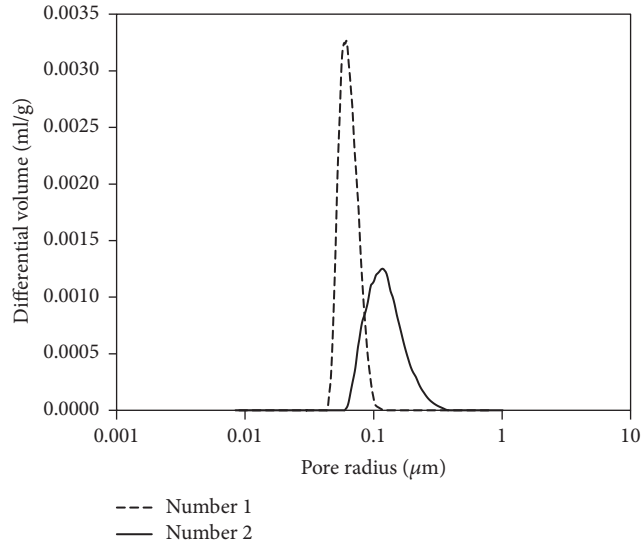

Figure 2: Pore size distribution of Jinping marble.

Table 2: Test results on flow rate of sample D30 in different conditions.

Sample D30: hydrostatic pressure: 20 MPa, room temperature: 15.0°C					
15.0°C		30.0°C		40.0°C	
Inlet gas pressure/MPa	Flow velocity/(10^{-3} mL·s^{-1})	Inlet gas pressure/MPa	Flow velocity/(10^{-3} mL·s^{-1})	Inlet gas pressure/MPa	Flow velocity/(10^{-3} mL·s^{-1})
4.31	0.00321	4.21	0.00183	4.52	0.00064
5.35	0.00467	5.44	0.00284	5.43	0.00086
6.42	0.00641	6.5	0.00392	6.32	0.00114
7.57	0.00893	7.45	0.00515	7.33	0.00149

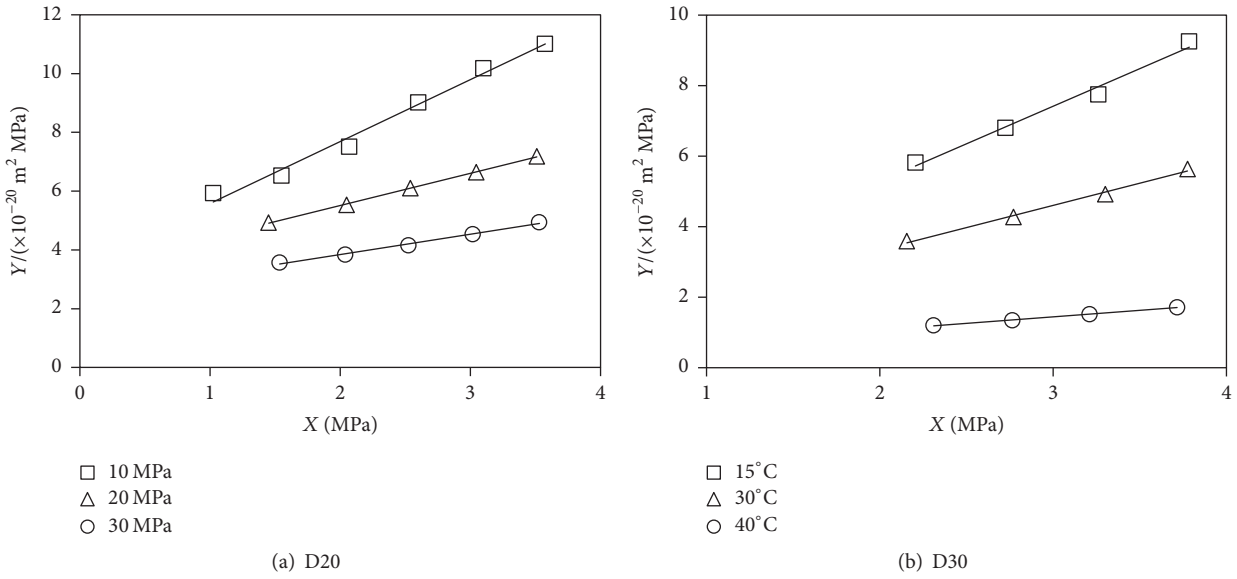

(a) D20 (b) D30

Figure 3: Fitting curve of test results for samples D20 and D30 by (3) (in the figure, $X = (p_0 + p_L)/2$ and $Y = Q_{v,r}p_rL\mu T_o/AT_r(p_0 - p_L)$).

in 1941 found that the permeability of a medium to gas is higher than that to liquid, and he attributed this phenomenon to "slip flow" between gas molecules and the pore wall surfaces. In Darcy flow, the collision between molecules and pore walls is negligible, and the flow velocity of the liquid is approximated as zero on the pore walls. However, the additional flux due to gas flow at the wall surfaces effectively increases as the pore radius approaches the mean free path of the gas molecules [2, 29]. This effect is expressed as follows:

$$K_g = K\left(1 + \frac{b}{p}\right), \tag{1}$$

where p is the average pore pressure and b is the Klinkenberg coefficient, which is related to pore geometry only.

The average pore pressure is often considered as the mean value of the inlet and outlet pressures and (1) can be expressed as follows:

$$K_g = K\left(1 + \frac{b}{(p_0 + p_L)/2}\right), \tag{2}$$

where p_0 and p_L are the inlet and outlet pressures, respectively.

The use of $(p_0 + p_L)/2$ in (2) is a rough estimation of the average gas pressure in the sample. Wu et al. [30] developed an analytical solution to estimate the permeability that incorporates the Klinkenberg effect. This solution is applicable when the sample temperature equals to the ambient air temperature. For tests performed on the sample D30, the sample temperature is different from the ambient air temperature, and the solution of Wu et al. [30] can be extended into

$$\frac{Q_{v,r}p_rL\mu}{A(p_0 - p_L)}\frac{T_o}{T_r} = Kb + K\frac{(p_0 + p_L)}{2}, \tag{3}$$

where L (m) and A (m^2) are the length and cross-sectional area of the test sample. T_r and $Q_{v,r}$ (m^3/s) are the room temperature and the volumetric flux under room conditions. μ is the gas viscosity (Pa·s). T_o is the sample temperature.

During testing, the outlet pressure p_L is kept constant while p_0 is varied and $Q_{v,r}$ is measured. Then, K and b are evaluated by fitting results according to (3). Figure 3 illustrates the fitting curves in which $Y = Q_{v,r}p_rL\mu T_o/AT_r(p_0 - p_L)$ is plotted against $X = (p_0 + p_L)/2$. K equals the slope of the fitting line and Kb is the value of y intercept. The permeability, Klinkenberg coefficient, and correlation coefficient R^2 are listed in Table 3. The results show that the Klinkenberg coefficient (b) increases as the permeability

Table 3: Fitting results of permeability and Klinkenberg coefficient of samples D20 and D30.

Sample	Pressure or temperature	$K/(10^{-21}\ \mathrm{m}^2)$	b/MPa	R^2
D20	10 MPa	21.1	1.64	0.993
	20 MPa	11.0	3.02	0.999
	30 MPa	6.92	3.55	0.994
D30	15°C	21.3	0.47	0.993
	30°C	12.6	0.67	0.998
	40°C	3.68	0.93	0.999

(K) decreases. It follows the same trend as the results from Tanikawa and Shimamoto [31].

The permeability of Jinping marble decreases as the pressure and temperature increase. The permeability decreases from $21.1 \times 10^{-21}\ \mathrm{m}^2$ to $6.92 \times 10^{-21}\ \mathrm{m}^2$ as the pressure increases from 10 to 30 MPa; the decrease range is 67.2%. And it decreases from $21.3 \times 10^{-21}\ \mathrm{m}^2$ to $3.68 \times 10^{-21}\ \mathrm{m}^2$ as the temperature increases from 15 to 40°C; the decrease range is 82.7%. Comparing with the influence of the moderate pressure on the permeability, the effect of temperature on the hydraulic property of tight rock is substantial.

4. Microphysical Model and Test Results Analysis

4.1. Microphysical Model. A significant number of studies have focused on developing the permeability evolution law in the dilatant regime based on percolation theory [32–34] or linear elastic fracture mechanics [35]. Little attention has been paid to permeability evolution in the compressive regime. In this study, the measured outflow of gas indicates the preexistence of linkage network of cracks in the samples. The variation of permeability during compression is due to the change of crack apertures.

Dienes [32] employed the continuum-averaging method and Poiseuille's law for laminar flow between parallel plates to develop an analytical result for the permeability tensor of rock intersected by isotropically distributed penny-shaped cracks. The permeability tensor is isotropic and is expressed as follows:

$$K = \frac{8\pi^2}{15}\theta\overline{A}^3 N_0 \bar{c}^5, \tag{4}$$

where θ accounts for the deviations of the crack shape from a uniform lamina, containing the drag effects of crack shape, crack end, and the roughness, $\overline{A}$ is the mean aspect ratio ($\overline{w}/\bar{c}$, where $\overline{w}$ is the mean crack half aperture (m) and $\bar{c}$ is the mean crack radius (m)) of the cracks, and N_0 denotes the number of cracks per unit volume that are not isolated.

Suppose the porosity (ϕ) of rock sample is composed of penny-shaped cracks which were due to rock damage during tectonic processes, sample collection, preparation, and so forth. It can be estimated from the mean crack aperture, radius, and spacing as follows [36]:

$$\phi = 2\pi\alpha\frac{\bar{c}^2\overline{w}}{\bar{l}^3}, \tag{5}$$

where $\bar{l}$ is the mean crack spacing (m) and α is the volumetric shape factor giving the deviation in volume from the ideal penny-shaped crack, defined as (real crack volume)/(ideal penny-shaped crack volume).

The connection between the permeability and the porosity (ϕ) is easily obtained from (4) and (5):

$$K = \frac{\theta N_0}{15\pi\alpha^3}\cdot\left(\frac{\bar{l}^3}{\bar{c}^2}\right)^3\cdot\phi^3. \tag{6}$$

In the compressive regime, the values of N_0, $\bar{l}$, $\bar{c}$, and α in (6) remain unchanged because no new microcrack initiates and propagates. The value of θ may change during compression. However, considering the averaging effect of many cracks, θ is assumed to be constant here. Therefore, the item $(\theta N_0/15\pi\alpha^3)\cdot(\bar{l}^3/\bar{c}^2)^3$ is considered as a constant during compression, and it is defined as β, which has no relations to the apertures of cracks. So, (6) can be written as

$$K = \beta\phi^3. \tag{7}$$

Equation (7) establishes the relationship between the permeability and the porosity (ϕ). It should be noted here that when crack propagates or new crack initiates, the value of β is no longer a constant.

4.2. Test Results Analysis. It is impossible to measure the porosity directly during testing. However, the value of porosity (ϕ) can be estimated from the initial porosity ϕ_0, volumetric strain ε_v, and mineral compressibility C_s:

$$\phi = \phi_0 - \varepsilon_v + C_s P. \tag{8}$$

So, (7) can be written as

$$K = \beta\left(\phi_0 - \varepsilon_v + C_s P\right)^3. \tag{9}$$

It can be seen from (9) that the intrinsic permeability decreases following a cubic relationship as the compressive volumetric strain increases.

The solid line in Figure 4 presents the volumetric strain of sample D20 as pressure increases. In (9), the compressibility (C_s) of dolomite can be obtained from its bulk modulus [37], and its value is 1.06×10^{-5}/MPa. The compressive volumetric strains (ε_v) at 10 MPa, 20 MPa, and 30 MPa are obtained from the volumetric strain curve in Figure 4, and they are $\varepsilon_{v10} = 0.00071$, $\varepsilon_{v20} = 0.0011$, and $\varepsilon_{v30} = 0.0013$, respectively. Combining the permeability test results (K in Table 3) at

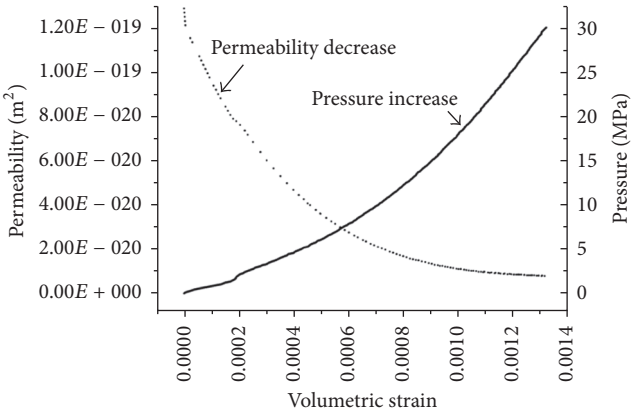

Figure 4: Permeability variation with volumetric strain during compression.

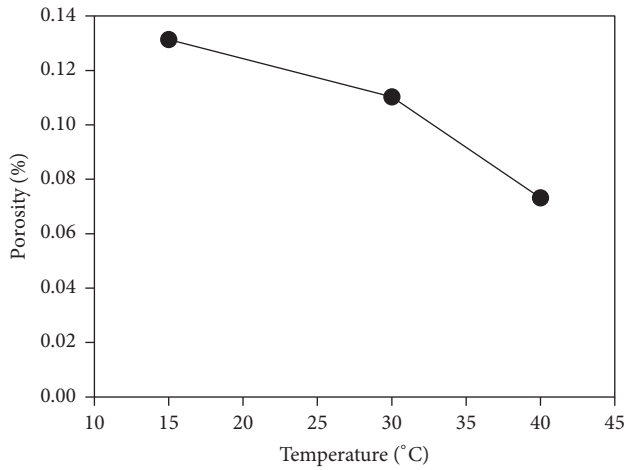

Figure 5: Variation of porosity with temperature under hydrostatic stress (20 MPa) for Jinping marble.

10 MPa, 20 MPa, and 30 MPa confining pressures (P), the parameters of β and ϕ_0 can be fitted from (9).

$$\beta = 0.94 \times 10^{-11}\ \mathrm{m}^2, \qquad \phi_0 = 0.19 \times 10^{-2}. \tag{10}$$

The initial porosity ϕ_0 determined from (9) is close to the intrusion test results (0.17% and 0.14%). Equation (9) can be used to predict variation of rock permeability from the variation of volumetric strain. The estimated permeability curve for D20 is plotted against volumetric strain in Figure 4 as the dot line. It should be noted that the linear Hook's law should not be applied to calculate the volumetric strain because the permeability variation law is based on the variation of crack aperture other than the elastic deformation of matrix. Replacing β in (7), the porosity can be estimated and it decreases from 0.13% to 0.09% as the pressure increases from 10 MPa to 30 MPa; the decrease range is 31%.

For D30, the permeability variation with temperature can be estimated by replacing the term $C_s P$ in (9) with $\alpha(T - T_0)$, where α is the thermal expansion coefficient of the mineral; T and T_0 are the current temperature and initial temperature. In the current test, the volumetric strains are not measured at different temperatures. So, the parameters β cannot be obtained from the test results of D30. Supposing that samples D30 and D20 have the same value of β, which means that cracks in both specimen follow the same distribution, the variation of porosity ϕ with temperatures can be roughly estimated from (7), as shown in Figure 5. The results show that the porosity decreases from 0.13% to 0.07% as the temperature increases from 15°C to 40°C; the decrease range is 44%. Equation (5) shows that the mean crack aperture ($2\overline{w}$) changes linearly with the porosity. Thus, the mean aperture also decreases 44% as temperature increases from 15°C to 40°C. The porosity change due to the thermal effect is also found by Sun et al. [38], who found that the porosity of granite decreases (from 0.88% to 0.75%) as temperature increases (from 25°C to 50°C) in the moderate temperature range. Comparing with the influence of the moderate pressure on the permeability presented above, the thermal effect on the permeability is notable and it should be taken into account into the estimation of the transport properties of intact rock.

5. Conclusions

The steady state method is used to study the permeability of Jinping marble under moderate pressures and temperatures in the compressive regime. The experimental results show that the permeability of Jinping marble decreases from 21.1 $\times 10^{-21}$ m^2 to 6.92 $\times 10^{-21}$ m^2 as the pressure increases from 10 to 30 MPa and decreases from 21.3 $\times 10^{-21}$ m^2 to 3.68 $\times 10^{-21}$ m^2 as the temperature increases from 15 to 40°C. The results imply that the influence of temperature on marble permeability is as remarkable as stress.

The permeability evolution law in the compressive regime is studied based on a geometric model of the penny-shaped crack distribution. The analytical result shows that the permeability decreases following a cubic law. The initial porosity of the marble estimated from the permeability tests is 0.19%, which is close to the results of the mercury intrusion porosimetry (0.14% and 0.17%). The analytical results show that the porosity decreases from 0.13% to 0.09% as the pressure increases from 10 MPa to 30 MPa, and from 0.13% to 0.07% as the temperature increases from 15°C to 40°C. From the permeability evolution law, the permeability for crystalline rock in the compressive regime due to moderate pressure and temperature can be estimated from the volumetric strain curve. The proposed permeability variation law will be furtherly verified to investigate the effect of moderate stress and temperature on the transport properties of host rock of underground nuclear waste repository in the future.

Conflicts of Interest

The authors declare that they have no conflicts of interest.

Acknowledgments

The authors gratefully acknowledge the support of the Chinese Fundamental Research (973) Program through Grant no. 2013CB03600.

References

[1] P. Cosenza, M. Ghoreychi, B. Bazargan-Sabet, and G. de Marsily, "In situ rock salt permeability measurement for long term safety assessment of storage," *International Journal of Rock Mechanics & Mining Sciences*, vol. 36, no. 4, pp. 509–526, 1999.

[2] D. Yang, W. Wang, W. Chen, S. Wang, and X. Wang, "Experimental investigation on the coupled effect of effective stress and gas slippage on the permeability of shale," *Scientific Reports*, vol. 7, Article ID 44696, 2017.

[3] C.-F. Tsang, F. Bernier, and C. Davies, "Geohydromechanical processes in the excavation damaged zone in crystalline rock, rock salt, and indurated and plastic clays—in the context of radioactive waste disposal," *International Journal of Rock Mechanics and Mining Sciences*, vol. 42, no. 1, pp. 109–125, 2005.

[4] Y. Chen, S. Hu, K. Wei, R. Hu, C. Zhou, and L. Jing, "Experimental characterization and micromechanical modeling of damage-induced permeability variation in Beishan granite," *International Journal of Rock Mechanics and Mining Sciences*, vol. 71, pp. 64–76, 2014.

[5] P. A. Witherspoon and J. E. Gale, "Mechanical and hydraulic properties of rocks related to induced seismicity," *Engineering Geology*, vol. 11, no. 1, pp. 23–55, 1977.

[6] M. A. Etheridge, V. J. Wall, S. F. Cox, and R. H. Vernon, "High fluid pressures during regional metamorphism and deformation: implications for mass transport and deformation mechanisms," *Journal of Geophysical Research*, vol. 89, no. 6, pp. 4344–4358, 1984.

[7] J. J. Ague, "Models of permeability contrasts in subduction zone mélange: implications for gradients in fluid fluxes, Syros and Tinos Islands, Greece," *Chemical Geology*, vol. 239, no. 3-4, pp. 217–227, 2007.

[8] N. J. C. Farrell, D. Healy, and C. W. Taylor, "Anisotropy of permeability in faulted porous sandstones," *Journal of Structural Geology*, vol. 63, pp. 50–67, 2014.

[9] S. Kolzenburg and J. K. Russell, "Welding of pyroclastic conduit infill: a mechanism for cyclical explosive eruptions," *Journal of Geophysical Research: Solid Earth*, vol. 119, no. 7, pp. 5305–5323, 2014.

[10] P. F. Boulin, P. Bretonnier, N. Gland, and J. M. Lombard, "Contribution of the steady state method to water permeability measurement in very low permeability porous media," *Oil and Gas Science and Technology*, vol. 67, no. 3, pp. 387–401, 2012.

[11] E. W. Bolton, A. C. Lasaga, and D. M. Rye, "Long-term flow/chemistry feedback in a porous medium with heterogenous permeability: kinetic control of dissolution and precipitation," *American Journal of Science*, vol. 299, no. 1, pp. 1–68, 1999.

[12] J.-J. Dong, J.-Y. Hsu, W.-J. Wu et al., "Stress-dependence of the permeability and porosity of sandstone and shale from TCDP Hole-A," *International Journal of Rock Mechanics and Mining Sciences*, vol. 47, no. 7, pp. 1141–1157, 2010.

[13] A. Kožušníková and P. Konečný, "Influence of temperature on the permeability of rocks," *Géotechnique*, vol. 61, no. 12, pp. 1081–1085, 2011.

[14] J. Chen, X. Yang, Q. Duan, and C. Peach, "Integrated measurements of permeability, effective porosity, and specific storage of core samples using water as the pore fluid," *International Journal of Rock Mechanics and Mining Sciences*, vol. 79, pp. 55–62, 2015.

[15] T. D. Rathnaweera, P. G. Ranjith, and M. S. A. Perera, "Effect of salinity on effective CO_2 permeability in reservoir rock determined by pressure transient methods: an experimental study on hawkesbury sandstone," *Rock Mechanics and Rock Engineering*, vol. 48, no. 5, pp. 2093–2110, 2015.

[16] P. Xu and S.-Q. Yang, "Permeability evolution of sandstone under short-term and long-term triaxial compression," *International Journal of Rock Mechanics and Mining Sciences*, vol. 85, pp. 152–164, 2016.

[17] L. L. Wang, G. Q. Zhang, S. Hallais, A. Tanguy, and D. S. Yang, "The swelling of shales: a multi-scale experimental investigation," *Energy & Fuels*, 2017.

[18] M. Souley, F. Homand, S. Pepa, and D. Hoxha, "Damage-induced permeability changes in granite: a case example at the URL in Canada," *International Journal of Rock Mechanics and Mining Sciences*, vol. 38, no. 2, pp. 297–310, 2001.

[19] O. Schulze, T. Popp, and H. Kern, "Development of damage and permeability in deforming rock salt," *Engineering Geology*, vol. 61, no. 2-3, pp. 163–180, 2001.

[20] T. Jiang, J. F. Shao, W. Y. Xu, and C. B. Zhou, "Experimental investigation and micromechanical analysis of damage and permeability variation in brittle rocks," *International Journal of Rock Mechanics and Mining Sciences*, vol. 47, no. 5, pp. 703–713, 2010.

[21] S. Chaki, M. Takarli, and W. Agbodjan, "Influence of thermal damage on physical properties of a granite rock: porosity, permeability and ultrasonic wave evolutions," *Construction and Building Materials*, vol. 22, no. 7, pp. 1456–1461, 2008.

[22] V. M. Shmonov, V. M. Vitovtova, and A. V. Zharikov, "Experimental study of seismic oscillation effect on rock permeability under high temperature and pressure," *International Journal of Rock Mechanics and Mining Sciences*, vol. 36, no. 3, pp. 405–412, 1999.

[23] A. V. Zharikov, V. M. Vitovtova, V. M. Shmonov, and A. A. Grafchikov, "Permeability of the rocks from the Kola superdeep borehole at high temperature and pressure: implication to fluid dynamics in the continental crust," *Tectonophysics*, vol. 370, no. 1-4, pp. 177–191, 2003.

[24] S. Chen, C. Yang, and G. Wang, "Evolution of thermal damage and permeability of Beishan granite," *Applied Thermal Engineering*, vol. 110, pp. 1533–1542, 2017.

[25] C. E. Manning and S. E. Ingebritsen, "Permeability of the continental crust: implications of geothermal data and metamorphic systems," *Reviews of Geophysics*, vol. 37, no. 1, pp. 127–150, 1999.

[26] A. P. S. Selvadurai and P. Carnaffan, "A transient pressure pulse method for the measurement of permeability of a cement grout," *Canadian Journal of Civil Engineering*, vol. 24, no. 3, pp. 489–502, 1997.

[27] X. Zhao, J. Zuo, and J. Pei, "Meso-experimental study of fracture mechanism of bedded marble in Jinping," *Chinese Journal of Rock Mechanics and Engineering*, vol. 31, no. 3, pp. 534–542, 2012.

[28] K. Malaga-Starzec, J. E. Lindqvist, and B. Schouenborg, "Experimental study on the variation in porosity of marble as a function of temperature," *Geological Society Special Publication*, vol. 205, no. 1, pp. 81–88, 2002.

[29] F. A. C. Dullien, *Porous Media, Fluid Transport and Pore Structure*, Academic Press, New York, NY, USA, 2nd edition, 1992.

[30] Y.-S. Wu, K. Pruess, and P. Persoff, "Gas flow in porous media with klinkenberg effects," *Transport in Porous Media*, vol. 32, no. 1, pp. 117–137, 1998.

[31] W. Tanikawa and T. Shimamoto, "Comparison of Klinkenberg-corrected gas permeability and water permeability in sedimentary rocks," *International Journal of Rock Mechanics and Mining Sciences*, vol. 46, no. 2, pp. 229–238, 2009.

[32] J. K. Dienes, "Permeability, percolation and statistical crack mechanics," in *Issues in Rock Mechanics*, R. E. Goodman and F. E. Heuze, Eds., 94, p. 86, American Institute of Mining, Metallurgical and Petroleum Engineers, New York, NY, USA, 1982.

[33] Y. Gueguen and J. Dienes, "Transport properties of rocks from statistics and percolation," *Mathematical Geology*, vol. 21, no. 1, pp. 1–13, 1989.

[34] W. Zhu and T.-F. Wong, "Network modeling of the evolution of permeability and dilatancy in compact rock," *Journal of Geophysical Research: Solid Earth*, vol. 104, no. 2, pp. 2963–2971, 1999.

[35] G. Simpson, Y. Guéguen, and F. Schneider, "Permeability enhancement due to microcrack dilatancy in the damage regime," *Journal of Geophysical Research: Solid Earth*, vol. 106, no. 3, pp. 3999–4016, 2001.

[36] C. J. Peach and C. J. Spiers, "Influence of crystal plastic deformation on dilatancy and permeability development in synthetic salt rock," *Tectonophysics*, vol. 256, no. 1-4, pp. 101–128, 1996.

[37] T. J. Ahrens, *Mineral Physics & Crystallography: A Handbook of Physical Constants*, Amer Geophysical Union, Washington, DC, USA, 1995.

[38] Q. Sun, W. Zhang, L. Xue, Z. Zhang, and T. Su, "Thermal damage pattern and thresholds of granite," *Environmental Earth Sciences*, vol. 74, no. 3, pp. 2341–2349, 2015.